Atmos. Chem. Phys. Discuss., 13, C9986–C10002, 2013
www.atmos-chem-phys-discuss.net/13/C9986/2013/

Atmospheric Chemistry and Physics Discussions

Interactive comment on "NAT nucleation and denitrification in the Arctic stratosphere" *by* J.-U. Grooß et al.

J.-U. Grooß et al.

j.-u.grooss@fz-juelich.de

Received and published: 13 December 2013

Reply to Reviewer 1

We thank the reviewer for the constructive comments. We agree with the majority of the typographical and stylistic and other suggestions and have changed them in the revised version as suggested. These points are not repeated here. The remaining points are explained below in detail.

on abstract: Equilibrium schemes are used in models as parametrisation. They do not take into account the supersaturation history of the individual air masses or

particles. These simpler schemes may provide reasonable values for chlorine activation and thus also for ozone depletion, if they are tuned to provide reasonable denitrification. Nevertheless we argue that the proposed mechanism is better suited to simulate NAT PSCs, as it is physically based.

on P22112/L24: The critical Lyapunov exponent is a measure of the strength of the mixing that is explained in detail in the papers of McKenna et al. (2002) and Konopka et al. (2004). Basically it defines a critical wind shear above which the CLaMS mixing algorithm is triggered. According to these studies, a meaningful parameter range should be between 1.2 and 1.5 day^{-1}, a value of 1.5 day^{-1} means lower mixing intensity which was e.g. used by Riese et al. (2012). This relevant parameter of the model setup should be documented here, however for its explanation we refer to the cited papers and clarify this in the revised paper.

on P22113/L16: The JPL evaluation does not consider the Plenge equilibrium constant. That is why it is mentioned here. It is now mentioned in the revised version that the recommendation of Suminska-Ebersoldt et al. are based on Geophysica observations.

on P22119/L5: The shown deviation below about 380 K is not so relevant for the results of the paper, therefore we re-formulate this sentence in this respect as suggested. Part of the deviation may be due to the vertical resolution of ACE-FTS.

on P22120/L26: One has to make a compromise. If the volume is too low and contains no or only 1-2 particle parcels, a meaningful particle size distribution cannot be derived; If the volume is too large, the derived average size distribution would smooth out the local structures. The volume size was chosen such that it is comparable to the model resolution. We changed this to 50 km for all cases which still get not too much noise and makes the different panels of Fig. 6 and 7 more comparable. This is clarified in the text of the revised version.

ACPD
13, C9986–C10002, 2013

on P22123/L8: Due to the coverage of ACE-FTS, the frequency of observations in the polar vortex varies with time. In the considered time periods there are always observation days with more than 10% of the stratospheric observations (between 20 and 25 km) inside the vortex core. Before 2 January, there are no vortex observations at all, such that we now state "This is the first time period during the simulation where ACE-FTS observations for the vortex core are available due to latitude coverage of the satellite."

on P22124/L21: Yes, the ERA-Interim data are available 6-hourly. So the deviations can either be caused by temperature fluctuations in between the 6-hourly time step or by structures not resolved in the ERA-Interim data. This 6-hourly availability of ERA-Interim data is mentioned in the revised version.

on P22126/L10f: Generally the importance of denitrification on ozone depletion is known. As the shown impact of different nucleation rate parametrisation on vortex average denitrification is rather low, the resulting impact on ozone is also anticipated to be low. However we see this not as an argument for not improving the simulation of the NAT particles.

on Figure 11: At the highest altitudes in the plot, the NO_y (and other tracer) mixing ratios are strongly influenced by the upper boundary at 900 K potential temperature. As there are no global data of NO_y available for defining the upper boundary continuously, it has to be derived from the correlation reported in Table A2 from N_2O. This method has some limitations as the correlation is not so compact for the upper altitudes (i.e. for low N_2O mixing ratios). This is also visible in the HNO_3 comparison (Figure 4). We added this explanation to the revised paper.

ACPD
13, C9986–C10002, 2013

Reply to Reviewer 2 / Stephan Fueglistaler

A major concern is that the comparison is based on one winter only and that the main comparison consists only of two orbits that are displayed in Figs. 5 and 6. We agree that the comparison between CALIPSO and CLaMS should be based on a statistical analysis. However, a repetition of this analysis for different winters would require a new setup of the initialisation and boundary condition as described for the winter 2009/2010 in detail. We feel that this is beyond the scope of this paper. However, the revised manuscript is improved in that respect by including repetition of the shown comparison for all orbits in the time range 21-30 December and a statistical comparison of these results. This comparison is based on the observations of backscatter ratio and perpendicular signal itself and its uncertainty.

on P22109/L25ff: While the NAT particles of all sizes contribute to the denitrification, the large particles dominate the flux. In the simulation, half of the HNO_3 flux is caused by the particles that have radii larger than 70% of the maximum radius $r_{\max}$. Although $r_{\max}$ varies with time it can be said that "...the largest particles with diameters above about 10 µm dominate the denitrification."

on P22111/L12ff: To clarify this point, We changed the paragraph about other studies using the same CLaMS run as follows:
"In addition to the present study, CLaMS has been used in a very similar configuration, however with a constant NAT nucleation rate, in several other recent works examining the Arctic winter of 2009/2010. For example, Hösen (2013) investigated in-situ tracer observations, while Woiwode (2013) and Kalicinsky et al. (2013) used CLaMS to interpret the remote sensing observations of the aircraft instruments MIPAS-ENVISAT and CRISTA-NF, respectively."

Further, Wohltmann et al. (2013) performed simulations with a focus on the sensitivity of polar chlorine chemistry and ozone loss on heterogeneous reactions,

ACPD
13, C9986–C10002, 2013

also using a constant NAT nucleation rate. Wohltmann et al. (2013) concluded that changes in the underlying assumptions on chlorine activation have only a small impact on the modelled ozone loss. This result confirms the finding by Wegner et al. (2012) and Drdla and Müller (2012) that substantial chlorine activation occurs on cold binary aerosols. However, uncertainties in NAT microphysics contribute most to the overall uncertainty in modeling heterogeneous chemistry and even though an increase in surface area due to NAT particles is of minor importance for modeling heterogeneous chemistry, the removal of reactive nitrogen due to denitrification remains important as it slows down or even inhibits chlorine deactivation."

on P22113/L1: Indeed, the effect of unresolved temperature resolutions depends upon the accuracy and resolution of the meteorological analysis. Hoyle et al. (2013) offered two sets of model parameters for use in models with and without a representation of small-scale temperature fluctuations. A coarse resolution of the underlying meteorological analysis requires a lower nucleation barrier for NAT to account for missing temperature minima and maxima and higher cooling rates resulting into partitioning effects between water and nitric acid, which could enhance NAT saturation ratios. Since CLaMS makes use of the ERA-Interim temperature fields and therefore does not account for small-scale fluctuations in the temperature data, the corresponding set of parameters has been chosen from Hoyle et al. (2013). The derived look-up tables need indeed an update once the quality of the meteorological analysis changes. However, focusing on NAT nucleation, the variance added is small and stated in Hoyle et al. (2013). Once the meterological model reaches the resolution of the waves added in Hoyle et al. (2013) (and described in Engel et al. (2013)), the explicit wave version of the nucleation parameterisation could be used.

on P22114/L1ff: We would like to point out that the interaction of particle growth, gas phase depletion as well as sedimentation is included in CLaMS even though the

ACPD
13, C9986–C10002, 2013

resolution is considerably lower than in the microphysical model used in the study by Fueglistaler et al. (2002). However, we realized that we should extend the discussion about different NAT formation pathways. Also in respond to the last two comments of this review, we should emphasize that there is probably not the only correct nucleation but several pathways to form NAT, which coexist, but which are not all accounted for in this work. The parametrisation, adopted from Hoyle et al. (2013) and included in CLaMS within this study, explains NAT formation in December prior to the existence of ice clouds. As deducible from the CALIOP observations from December 2009, NAT number densities remain in the order of 10^{-3} to 10^{-4} cm^{-3} (Pitts et al., 2011) and the parametrisation from Hoyle et al. (2013) coincides with these measurements. High number density NAT clouds, which can act as mother clouds for "NAT-rocks", cannot be reproduced with this approach. An adjustment of the parametrisation towards higher NAT number densities would worsen the agreement with the December observations. High number density NAT clouds most likely originate from ice clouds as originally proposed by Carslaw et al. (1998b) and later parametrised by Luo et al. (2003). Also in the Arctic winter 2009/2010, high number density NAT clouds have been observed only after the occurrence of ice PSCs within the vortex (Pitts et al., 2011; Engel et al., 2013). The implementation of ice nucleation together with a parametrisation of high number density NAT clouds into CLaMS as described by Engel et al. (2013) is beyond the scope of this paper but something we would like to address in the future.

on P22117/L1ff: We rewrote the paragraph starting on page 22116/L27:

"Tracing $S_{NAT}^{\max}$ and $T_{\min}$ along the air parcel trajectory has two reasons. First, $S_{NAT}^{\max}$ and $T_{\min}$ are evaluated on an hourly basis whereas the nucleation of NAT particles is decided on a daily basis. The higher time resolution improves the temperature information and increases the possibility to capture temperature minima or maxima. Second, each combination of $S_{NAT}^{\max}$ and $T_{\min}$ represents a certain

ACPD
13, C9986–C10002, 2013

contact angle bin and decides whether or not additional NAT particles are nucleated. Only if S_{NAT} increases above the value of $S_{NAT}^{\max}$ 24 hours before, additional NAT particles are nucleated. The number of NAT particles remains constant for $S_{NAT}^{\max}$ equal or smaller $S_{NAT}^{\max}$ 24 hours before. This is a major difference to the constant nucleation rate approach, which leads to a continuous formation of new particles as long as S_{NAT} is larger than unity. The nucleation rate is determined by summing up the tabulated particle concentrations in the bins of newly activated contact angles, which correspond to a certain combination of temperature and supersaturation (see Fig. 1). Figure 2..."

on P22117/L25ff: yes. We changed this paragraph to:

"Since the distribution of NAT particle sizes in the simulation is given by particle parcels each representing a single size, it is not clear whether the chosen density of the particle parcels does successfully represent the properties of all NAT particles. To examine this possible under-sampling, a simulation was performed in which the density of NAT particle parcels nucleated each day was increased from 4 to 64 per air parcel (S64). In turn, the corresponding density assigned to each particle parcel was decreased by a factor of 16."

We further left out the simulation X5 that didn't add much information to the discussion.

on P22118/L6: It is clear that the processes described here do have a strong temperature dependence. To illustrate the sensitivity of the results upon temperature changes we added a simulation in which the global temperatures were decreased by 1 K. In order to add to the picture, we also included the opposite sensitivity with temperatures increased by 1 K. We rewrite this part as

"Since the simulated nucleation and growth of the NAT particles strongly depend on temperature, we also include two sensitivity simulations, in which the ERA-Interim were decreased and increased by 1 K, respectively (T-1K and T+1K)."

ACPD
13, C9986–C10002, 2013

on P22119/Figure 4: We present water vapour (and HNO_3) mixing ratios here, because they are important for the determination of S_{NAT} and thus the derived nucleation rates. This is said at the beginning of section 3.1. To further clarify this point, we rewrite the last sentence of this sections as
"Since CLaMS is able to reproduce the observed H_2O and HNO_3 fields in the lower stratosphere, we expect no significant deviations of the derived nucleation rate or PSC properties due to the uncertainty in gas phase H_2O and HNO_3." Note that the shown model data are derived from the CLaMS points co-located with ACE-FTS.

on P22120/L1ff and L5ff: For the construction of a particle size distribution on the basis of this simulation one has to collect information from particle parcels over a sample volume. (This is similar to deriving a size distribution from in-situ FSSP measurements). Each particle parcel is assigned a particle density assumed to be constant over the volume of one air parcel in the model. The size distribution is then plotted by binning the collected particles into size bins. The choice of these bins was adjusted to those given by the FSSP. In the shown figure 38 particle parcels contribute to the shown NAT size distribution. The signal observed by FSSP should be the sum of the NAT and the STS peak. This is explained in more detail in the revised version.
Regarding the mis-match of the large particles, we should first point out that there is fair agreement for the particles with diameters below 10 µm. Indeed, there are discrepancies for the large particles observed by FSSP, which are not present in the simulation. This is mentioned in the paper, however, the reason for that is unclear. Possible biases in the detection of highly aspherical particle shapes are one speculation that may explain the discrepancy. We do think that we should mention this discrepancy and that presenting the FSSP data would not be pointless even though uncertainties exist for the largest particles diameters.

on P22120/L26: See corresponding answer to reviewer 1.

ACPD
13, C9986–C10002, 2013

on P22121/L8: We agree with Stefan Fueglistaler that the taken numerical values should be supported by references. The new paragraph is now as follows:

"From these particle size distributions, we calculated aerosol backscatter ratios and perpendicular backscatter signals using Mie and T-matrix calculations (Mishchenko et al., 2010). The refractive index for STS was assumed to be 1.44 (Krieger et al., 2000). For NAT, a fixed refractive index of 1.48 was chosen, as used in several earlier studies (Carslaw et al., 1998a; Voigt et al., 2003; Luo et al., 2003; Fueglistaler et al., 2003). However, this value is associated with uncertainty and the literature offers a slightly broader range of possible values (e.g. Middlebrook et al., 1994; Toon et al., 1994; Deshler et al., 2000; Biermann et al., 2000). Furthermore, we treat NAT particles as prolate spheroids with aspect ratios of 0.9 (diameter-to-length ratio). Liu and Mishchenko (2001) recommended an aspect ratio smaller 0.83, whereas Daerden et al. (2007) and Scarchilli et al. (2005) used 0.95. We achieve the best agreement with CALIOP measurements using an aspect ratio of 0.9, which yields high values of depolarization. Increasing asphericity, which is in our nomenclature equal to decreasing aspect ratios, results in lower values of the perpendicular backscatter coefficient (see Fig. 7 in Flentje et al., 2002). We performed further T-matrix calculations with aspect ratios of 0.8 and 0.7 (not shown). The agreement between CALIOP and the CLaMS simulations got worse with respect to the perpendicular backscatter, whereas a change in aspect ratio effects BSRs, often dominated by liquid particles, too a smaller degree."

on P22121/L17ff: Figure 5 and 6 are two exemplary orbits, one taken from the beginning of the NAT period in December 2009 and one taken from the last day before the first ice cloud has been detected in the polar vortex. We agree with the reviewer that CALIOP offers much more data for further comparisons. However, we would like to keep the two plots as exemplary orbits. The improvement by the new nucleation scheme in comparison to a constant nucleation rate is from our

ACPD
13, C9986–C10002, 2013

point of view clearly visibly. It should be noted that the two orbits were selected by chance and not because they showed the most prominent improvement.

To make use of all available CALIOP data from December 2009, we did a statistical comparison between CALIOP and CLaMS. This analysis clearly highlights the improvement of the new nucleation scheme in reproducing PSC occurrences. Therefore, we included a new figure into our manuscript, which we explained in an additional paragraph as follows:

"A comparison based on all available CALIOP data between 21 and 30 December 2009 is shown in the new Fig. 8. The top panel displays the ratio between the observed and simulated cloud fraction (CF) per day. On 21 December, the HR and LR simulations underestimate the observed CF. CF for T+1K is equal to zero until 25 December. On 21 December, Jconst already has a modelled area of PSC seven times greater than that observed. All simulations show a trend towards higher CF with proceeding time. On 30 December, all simulations overestimate the cloud coverage by at least a factor of two. The only exception is T+1K with a CF close to 0.5 (not visible in Fig. 8). The second and third panel of Fig. 8 illustrate a point-by-point comparison between CALIOP and CLaMS based on the backscatter ratio (BSR) and the perpendicular backscatter signal (β_{perp}). The level of agreement is expressed in terms of σ, which is the uncertainty associated to the CALIOP measurement. The uncertainty scales with the vertical and horizontal averaging of the data (Δ_{vertical} and $\Delta_{\text{horizontal}}$, respectively) and can be calculated for β as follows:

$$\sigma(\beta) = \frac{1}{75}\,\beta\,\sqrt{\frac{2.39\times10^{-5}\,\text{km}^{-1}\text{sr}^{-1}}{\beta}\times\frac{1500\,\text{km}}{\Delta_{\text{horizontal}}}\times\frac{5\,\text{km}}{\Delta_{\text{vertical}}}} \qquad (1)$$

(Hunt et al., 2009; Engel et al., 2013). This translates into an uncertainty for BSR of

ACPD
13, C9986–C10002, 2013

$$\sigma(\mathrm{BSR}) = \mathrm{BSR} \times \frac{\sqrt{\sigma^2(\beta_{\mathrm{perp}}) + \sigma^2(\beta_{\mathrm{para}})}}{\beta_{\mathrm{perp}} + \beta_{\mathrm{para}}}. \quad (2)$$

We determined the difference in BSR and β_{perp} between CALIOP and CLaMS for every data point separately and expressed this difference as a fraction of σ. Shown are daily median values for the different simulations. Only data points with temperatures less than 196 K have been considered to reduce the cloudless background. However, the ratio between cloudy and cloudless areas is still unbalanced and the median is dominated by the background values, which tend to be lower in the simulation than in the measurement. Nevertheless, the area covered by clouds increases towards the end of the month and so does the deviation between measurement and simulation. Most prominent is the increasing deviation from the expected value in the Jconst and T-1K simulations."

on P22122/L5ff: The HNO_3 flux differs in the different studies because of several reasons. In the beginning it is more determined by the nucleation rate, that means that a higher nucleation rate corresponds to a larger flux. Later in the winter, the formation of NAT may be slowed down as less HNO_3 is available. We added this to the corresponding section.

on P22122/L24: One would expect two regimes of particle densities in which an increase of the nucleation rate has different consequences. In the case of low NAT particle density where particles do not significantly compete for gas phase HNO_3, additional nucleation would increase the denitrification. In the case of high NAT particle density, additional nucleation has no large effect, even a reduction of denitrification would be possible. The shown results indicate that the simulation is in the first regime. This paragraph was re-written to clarify this:
"Differences in the HNO_3 flux in the beginning of the NAT period correspond to the differences in the nucleation rate such that a larger nucleation rate causes

ACPD
13, C9986–C10002, 2013

a larger flux. However, the formation of NAT may be slowed down later as less HNO_3 is available due to earlier denitrification. [...] Especially later in the winter, the difference between the different sensitivity simulations becomes smaller. This compensation is likely due to the fact that the formation of NAT may be slowed down for air masses with less available HNO_3 due to earlier denitrification."

on P22123/L5: The "average vortex value as observed by ACE-FTS" is shown, which is an average profile of all data with equivalent latitude $> 70°$ N within the given time interval. The CLaMS lines show the results at the ACE-FTS tangent points evaluated in the same manner. This was clarified in the revised manuscript

on P22124/L21: We agree that other reasons like not resolved NAT nucleation on ice particles (see above) may also complicate the simulation and the comparison here. This is mentioned in the text now.

on P22125/L19-20: The added statistical comparison (the new Fig. 8 and corresponding discussion) does clarify better the improvement of the introduced nucleation rate scheme. The comparisons show that the general behaviour of the observations is reproduced by the simulations. The location and extent of the observed NAT PSCs as seen in the CALIOP data are clearly better reproduced by the new nucleation scheme than by using a constant nucleation rate. The constant nucleation rate overestimates cloud coverage as well as single optical cloud properties significantly. However, the vortex averaged NO_y profiles observed by ACE-FTS can be reproduced by all model configurations. Differences between the simulations are visible in the temporal evolution of the NO_y flux, but the averaged NO_y profiles in late winter are very similar despite different nucleation mechanisms.

ACPD
13, C9986–C10002, 2013

Further remarks

We revised the manuscript on the basis of the two reviewer comments. As explained above we added a statistical comparison between CALIPSO and CLaMS results that should complement the study. We now show also a sensitivity study in which ERA-Interim temperatures were increased by 1K. In addition, we re-arranged some figures such that all sensitivity simulations are color-coded identical in all plots. For better readability of the SIOUX NO_y comparison, some lines corresponding to sensitivity runs were excluded for the last two figures.

References

Biermann, U. M., Luo, B. P., and Peter, T.: Absorption spectra and optical constants of binary and ternary solutions of H_2SO_4, HNO_3, and H_2O in the mid infrared at atmospheric temperatures, J. Phys. Chem. A, 104, 783–793, doi:10.1021/jp992349i, 2000.

Carslaw, K. S., Wirth, M., Tsias, A., Luo, B. P., Dörnbrack, A., Leutbecher, M., Volkert, H., Renger, W., Bacmeister, J. T., and Peter, T.: Particle processes and chemistry in remotely observed mountain polar stratospheric clouds, J. Geophys. Res., 103, 5785–5796, 1998a.

Carslaw, K. S., Wirth, M., Tsias, A., Luo, B. P., Dörnbrack, A., Leutbecher, M., Volkert, H., Renger, W., Bacmeister, J. T., Reimer, E., and Peter, T.: Increased Stratospheric Ozone Depletion Due to Mountain-Induced Atmospheric Waves, Nature, 391, 675–678, 1998b.

Daerden, F., Larsen, N., Chabrillat, S., Errera, Q., Bonjean, S., Fonteyn, D., Hoppel, K., and Fromm, M.: A 3D-CTM with detailed online PSC-microphysics: analysis of the Antarctic winter 2003 by comparison with satellite observations, Atmos. Chem. Phys., 7, 1755–1772, 2007.

Deshler, T., Nardi, B., Adriani, A., Cairo, F., Hansen, G., Fierli, F., Hauchecorne, A., and Pulvirenti, L.: Determining the index of refraction of polar stratospheric clouds above Andoya (69°N) by combining size-resolved concentration and optical scattering measurements, J. Geophys. Res., 105, 3943–3953, doi:10.1029/1999JD900469, 2000.

ACPD

13, C9986–C10002, 2013

Drdla, K. and Müller, R.: Temperature thresholds for chlorine activation and ozone loss in the polar stratosphere, Ann. Geophys., 30, 1055–1073, doi:10.5194/angeo-30-1-2012, 2012.
Engel, I., Luo, B. P., Pitts, M. C., Poole, L. R., Hoyle, C. R., Grooß, J.-U., Dörnbrack, A., and Peter, T.: Heterogeneous formation of polar stratospheric clouds - Part 2: Nucleation of ice on synoptic scales, Atmos. Chem. Phys., 13, 10 769–10 785, doi:10.5194/acp-13-10769-2013, 2013.
Flentje, H., Dörnbrack, A., Fix, A., Meister, A., Schmid, H., Fueglistaler, S., Luo, B. P., and Peter, T.: Denitrification inside the stratospheric vortex in the winter of 1999-2000 by sedimentation of large nitric acid trihydrate particles, J. Geophys. Res., 107, AAC 11–1–AAC 11–15, doi:10.1029/2001JD001015, 2002.
Fueglistaler, S., Luo, B. P., Voigt, C., Carslaw, K. S., and Peter, T.: NAT-rock formation by mother clouds: a microphysical model study, Atmos. Chem. Phys., 2, 93–98, 2002.
Fueglistaler, S., Buss, S., Luo, B. P., Wernli, H., Flentje, H., Hostetler, C. A., Poole, L. R., Carslaw, K. S., and Peter, T.: Detailed modeling of mountain wave PSCs, Atmos. Chem. Phys., 3, 697–712, 2003.
Hösen, E.: Untersuchung von Transport, Mischung und Ozonverlust in der arktischen Polarregion im Winter 2009/10 basierend auf flugzeuggestützten in-situ-Messungen, Dissertation, Bergische Universität Wuppertal, Germany, 2013.
Hoyle, C. R., Engel, I., Luo, B. P., Pitts, M. C., Poole, L. R., Grooß, J.-U., and Peter, T.: Heterogeneous formation of polar stratospheric clouds - Part 1: Nucleation of nitric acid trihydrate (NAT), Atmos. Chem. Phys., 13, 9577–9595, doi:10.5194/acp-13-9577-2013, 2013.
Hunt, W. H., Winker, D. M., Vaughan, M. A., Powell, K. A., Lucker, P. L., and Weimer, C.: CALIPSO Lidar Description and Performance Assessment, J. Atmos. Ocean. Technol., 26, 1214–1228, doi:{10.1175/2009JTECHA1223.1}, 2009.
Kalicinsky, C., Grooß, J.-U., Günther, G., Ungermann, J., Blank, J., Höfer, S., Hoffmann, L., Knieling, P., Olschewski, F., Spang, R., Stroh, F., and Riese, M.: Observations of filamentary structures near the vortex edge in the Arctic winter lower stratosphere, Atmos. Chem. Phys., 13, 10 859–10 871, 2013.
Konopka, P., Steinhorst, H.-M., Grooß, J.-U., Günther, G., Müller, R., Elkins, J. W., Jost, H.-J., Richard, E., Schmidt, U., Toon, G., and McKenna, D. S.: Mixing and Ozone Loss in the 1999-2000 Arctic Vortex: Simulations with the 3-dimensional Chemical Lagrangian Model of the Stratosphere (CLaMS), J. Geophys. Res., 109, D02315, doi:10.1029/2003JD003792, 2004.
Krieger, U. K., Mössinger, J. C., Luo, B. P., Weers, U., and Peter, T.: Measurement of the

refractive indices of H_2SO_4-HNO_3-H_2O solutions to stratospheric temperatures, Appl. Opt., 39, 3691–3703, doi:10.1364/AO.39.003691, 2000.
Liu, L. and Mishchenko, M. I.: Constraints on PSC particle microphysics derived from lidar observations, J. Quant. Spectrosc. Radiat. Transf., 70, 817–831, doi:10.1016/S0022-4073(01)00048-6, 2001.
Luo, B. P., Voigt, C., Fueglistaler, S., and Peter, T.: Extreme NAT supersaturations in mountain wave ice PSCs: A clue to NAT formation, J. Geophys. Res., 108, 4443, doi:10.1029/2002JD003104, 2003.
McKenna, D. S., Konopka, P., Grooß, J.-U., Günther, G., Müller, R., Spang, R., Offermann, D., and Orsolini, Y.: A new Chemical Lagrangian Model of the Stratosphere (CLaMS): 1. Formulation of advection and mixing, J. Geophys. Res., 107, 4309, doi:10.1029/2000JD000114, 2002.
Middlebrook, A. M., Berland, B. S., George, S. M., Tolbert, M. A., and Toon, O. B.: Real refractive indices of infrared-characterized nitric-acid/ice films: Implications for optical measurements of polar stratospheric clouds, J. Geophys. Res., 99, 25 655–25 666, doi:10.1029/94JD02391, 1994.
Mishchenko, M. I., Travis, L. D., and Mackowski, D. W.: T-matrix computations of light scattering by nonspherical particles: a review, J. Quant. Spectrosc. Radiat. Transf., 111, 1704–1744, 2010.
Pitts, M. C., Poole, L. R., Dörnbrack, A., and Thomason, L. W.: The 2009-2010 Arctic polar stratospheric cloud season: A CALIPSO perspective, Atmos. Chem. Phys., 11, 2161–2177, doi:10.5194/acp-11-2161-2011, 2011.
Riese, M., Ploeger, F., Rap, A., Vogel, B., Konopka, P., Dameris, M., and Forster, P.: Impact of uncertainties in atmospheric mixing on simulated UTLS composition and related radiative effects, J. Geophys. Res., 117, D16305, doi:10.1029/2012JD017751, 2012.
Scarchilli, C., Adriani, A., Cairo, F., Donfrancesco, G. D., Buontempo, C., Snels, M., Moriconi, M. L., Deshler, T., Larsen, N., Luo, B. P., Mauersberger, K., Ovarlez, J., Rosen, J., and Schreiner, J.: Determination of polar stratospheric cloud particle refractive indices by use of in situ optical measurements and T-matrix calculations, Appl. Opt., 44, 3302–3311, doi:10.1364/AO.44.003302, 2005.
Toon, O. B., Tolbert, M. A., Koehler, B. G., Middlebrook, A. M., and Jordan, J.: Infrared optical constants of H_2O ice, amorphous nitric acid solutions, and nitric acid hydrates, J. Geophys. Res., 99, 25 631–25 654, doi:10.1029/94JD02388, 1994.

Voigt, C., Larsen, N., Deshler, T., Kröger, C., Schreiner, J., Mauersberger, K., Luo, B., Adriani, A., Cairo, F., Di Donfrancesco, G., Ovarlez, J., Ovarlez, H., Dörnbrack, A., Knudsen, B., and Rosen, J.: In situ mountain-wave polar stratospheric cloud measurements: Implications for nitric acid trihydrate formation, J. Geophys. Res., 108, 8331, doi:10.1029/2001JD001185, 2003.

Wegner, T., Grooß, J.-U., von Hobe, M., Stroh, F., Sumińska-Ebersoldt, O., Volk, C. M., Hösen, E., Mitev, V., Shur, G., and Müller, R.: Heterogeneous chlorine activation on stratospheric aerosols and clouds in the Arctic polar vortex, Atmos. Chem. Phys., 12, 11 095–11 106, doi:10.5194/acp-12-11095-2012, 2012.

Wohltmann, I., Wegner, T., Müller, R., Lehmann, R., Rex, M., Manney, G. L., Santee, M. L., Bernath, P., Sumińska-Ebersoldt, O., Stroh, F., von Hobe, M., Volk, C. M., Hösen, E., Ravegnani, F., Ulanovsky, A., and Yushkov, V.: Uncertainties in modelling heterogeneous chemistry and Arctic ozone depletion in the winter 2009/2010, Atmos. Chem. Phys., 13, 3909–3929, 2013.

Woiwode, W.: Qualification of the airborne FTIR spectrometer MIPAS-STR and study on denitrification and chlorine deactivation in Arctic winter 2009/10, Dissertation, Karlsruhe Insitute for Technology, Faculty of Chemistry and Biosciences, Karlsruhe, Germany, 2013.

Interactive comment on Atmos. Chem. Phys. Discuss., 13, 22107, 2013.

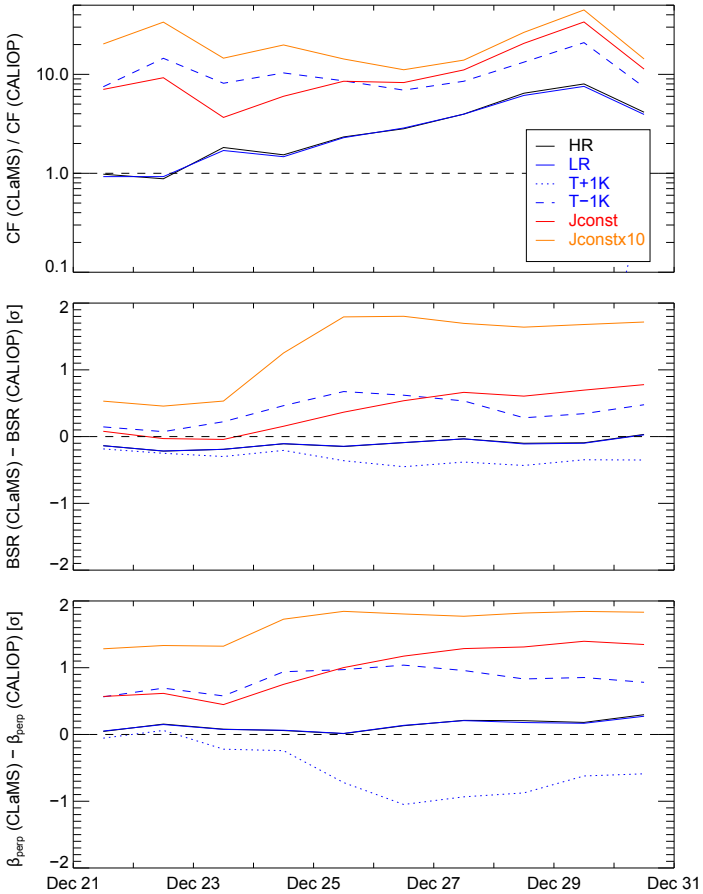

Fig. 1. Comparison of simulated optical properties by CLaMS with CALIOP. top: Ratio between observed and simulated cloud fraction (CF); middle/bottom: point-by-point comparison of CALIPSO signals (see text).

ACPD
13, C9986–C10002, 2013